Appl Phys B (2010) 98: 55–60
DOI 10.1007/s00340-009-3704-8

Applied Physics B
Lasers and Optics

805-nm diode-pumped continuous-wave 2-μm laser performance of Tm^{3+}:$BaGd_2(MoO_4)_4$ cleavage plate

Y.J. Chen · Y.F. Lin · X.H. Gong · H.M. Zhu · Z.D. Luo · Y.D. Huang

Received: 27 April 2009 / Revised version: 17 July 2009 / Published online: 12 September 2009

Abstract End-pumped by a single-stripe 805-nm diode laser, a maximum continuous-wave output power of 290 mW with slope efficiency of 42% and 90 mW with slope efficiency of 44% around 2 μm were achieved in a 1.6-mm-thickness, unprocessed 7.2 at.% Tm^{3+}:$BaGd_2(MoO_4)_4$ cleavage plate in a hemispherical and plano–plano cavities, respectively, when the absorbed pump power was 830 mW. The dependence of the polarization of output laser on the output coupler transmission was investigated. The influence of upconversion on the laser performance was analyzed. The results show that the unprocessed Tm^{3+}:$BaGd_2(MoO_4)_4$ cleavage plate is a promising 2-μm laser gain medium pumped by diode laser around 808 nm.

PACS 42.55.Rz · 42.55.Xi · 42.60.Pk · 42.70.Hj

1 Introduction

Because of the presence of many absorption lines of several chemical compounds (H_2O, CO_2, N_2O, etc.) in the spectral region around 2 μm, eye-safe Tm^{3+} solid-state lasers around 2 μm corresponding to the $^3F_4 \rightarrow {}^3H_6$ transition have attracted considerable attention and are important for various applications, such as medicine, remote sensing, environment gas detection, and high-resolution spectroscopy.

Y.J. Chen · Y.F. Lin · X.H. Gong · H.M. Zhu · Z.D. Luo · Y.D. Huang (✉)
Key Laboratory of Optoelectronic Materials Chemistry and Physics, Fujian Institute of Research on the Structure of Matter, Chinese Academy of Sciences, Fuzhou, Fujian, 350002, China
e-mail: huyd@fjirsm.ac.cn
Fax: +86-591-83715544

Pumping the Tm^{3+} ions into the $^3H_4$ level, efficient 2-μm lasers with slope efficiency higher than its Stokes limit (about 40%) have been realized in some Tm^{3+}-doped materials with appropriate Tm^{3+} concentration [1–4], because in theory one pump photon can excite two ions into the upper laser level $^3F_4$ finally through efficient cross-relaxation process between Tm^{3+} ions. However, since the peak absorption wavelength of the $^3H_6 \rightarrow {}^3H_4$ transition of Tm^{3+} ions in most crystals is shorter than 800 nm and the absorption of the transition is weak around 808 nm, Ti:sapphire laser or laser diode (LD) at wavelength shorter than 800 nm is adopted as the pump source for most of the Tm^{3+}-doped laser crystals presently [1, 4–6]. Therefore, taking into account the cheaper LD around 808 nm developed for Nd^{3+} lasers, a Tm^{3+}-doped laser crystal pumped effectively by LD around 808 nm is necessary for constructing an efficient and inexpensive all solid-state 2-μm laser [7, 8].

$BaGd_2(MoO_4)_4$(BGM) crystal belongs to the monoclinic structure and has a perfect (010) cleavage plane [9]. Because it melts congruently at about 1076°C, the crystal with large size and high optical quality can be easily grown by the Czochraski method in air [10, 11]. Detailed polarized spectroscopic properties of oriented Tm^{3+}:BGM crystal has been investigated [11]. Using an unprocessed Tm^{3+}:BGM cleavage plate as gain medium, which can avoid the cutting and polishing processes of the crystal and reduce the impurities on the surfaces, efficient quasi-continuous-wave (quasi-CW) 2-μm laser operation has also been demonstrated when it is pumped by a Ti:sapphire laser at 798 nm [11]. In this paper, CW 2-μm laser performance of a 1.6-mm-thick Tm^{3+}:BGM cleavage plate pumped by a single-stripe 805-nm LD is reported.

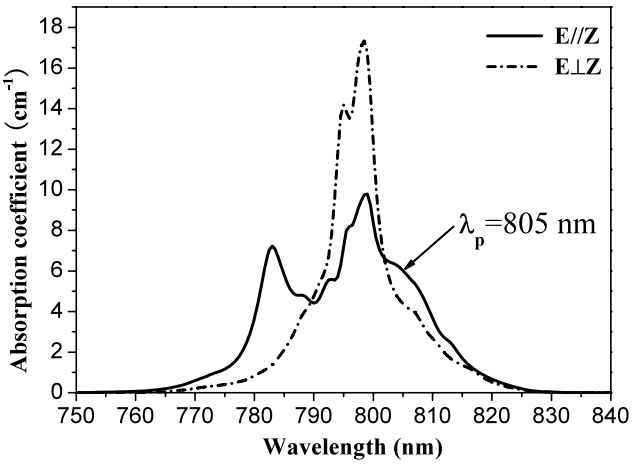

Fig. 1 Room-temperature polarized absorption spectra of the 7.2 at.% Tm^{3+}:BGM cleavage plate in a range of 750–840 nm

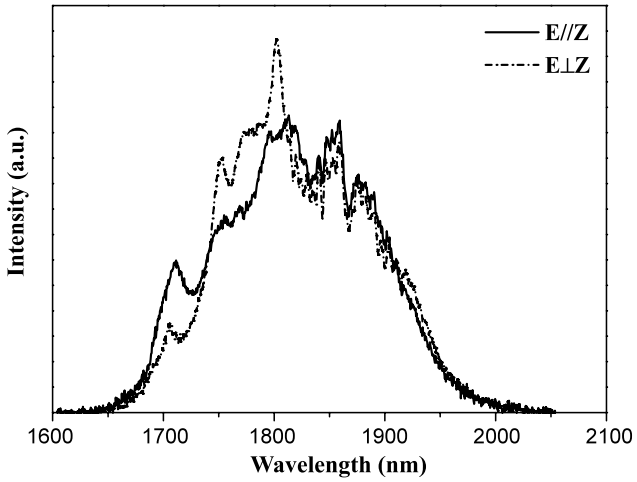

Fig. 2 Room-temperature polarized fluorescence spectra of the 7.2 at.% Tm^{3+}:BGM cleavage plate in a range of 1600–2100 nm

2 Spectral properties

A piece of unprocessed cleavage plate along the (010) cleavage plane directly obtained from an as-grown Tm^{3+}:BGM crystal using a knife was used in the spectral and laser experiments. The thickness of the plate is 1.6 mm. One principal axis Z of the optical indicatrix of the Tm^{3+}:BGM crystal is parallel to the (010) cleavage plane [11]. The room-temperature polarized absorption spectra of the cleavage plate in a range from 750 to 840 nm recorded with a spectrophotometer (Lambda 900, Perkin-Elmer) are shown in Fig. 1. The discrepancy of peak absorption coefficient at 798 nm for the polarization E of incident light parallel to the Z axis of the crystal ($E \parallel Z$) between this work (about 9.5 cm^{-1}) and Ref. [11] (about 8.5 cm^{-1}) may be mainly attributed to the inhomogeneity of the Tm^{3+} concentration in the different plates, though both of them were obtained from the same as-grown crystal. The inhomogeneous distribution of Tm^{3+} ions in a BGM crystal is caused by the nonunit segregation coefficient (about 0.8) [11]. According to the accurate Tm^{3+} concentration of 6.4 at.% measured in the plate of Ref. [11], the Tm^{3+} concentration of the cleavage plate used in this work was estimated to be about 7.2 at.% (4.6×10^{20} cm^{-3}). From Fig. 1 it can be seen that the absorption coefficients for $E \parallel Z$ in the range of 802−815 nm are larger than those for $E \perp Z$. The absorption coefficient at the pump wavelength of 805 nm for $E \parallel Z$ is 6 cm^{-1}, which is larger than those of 5 at.% Tm^{3+}:YAG (1 cm^{-1}) [7], 5.5 at.% Tm^{3+}:$YAlO_3$ (1–2 cm^{-1}) [12], and Tm^{3+}-doped fluoride crystals (such as 1 cm^{-1} for 12 at.% Tm^{3+}:BaY_2F_8) [4], but less than those of 5.6 at.% Tm^{3+}:$GdVO_4$ (8.5 and 11 cm^{-1} for π and σ polarizations, respectively) [7] and 6 at.% Tm^{3+}:$KY(WO_4)_2$ (about 10.5 cm^{-1} for $E \perp c$ polarization) [3] crystals at 805 nm. Furthermore, the absorption coefficient of the Tm^{3+}:BGM plate at 808 nm for $E \parallel Z$ is 5 cm^{-1}. The value is also larger than those of 5 at.% Tm^{3+}:YAG (about 0.5 cm^{-1}) [7], 5.5 at.% Tm^{3+}:$YAlO_3$ (1–2 cm^{-1}) [12], and Tm^{3+}-doped fluoride crystals (such as about 1 cm^{-1} for 12 at.% Tm^{3+}:BaY_2F_8) [4] at 808 nm. At the same time, it is comparable with those of 5.6 at.% Tm^{3+}:$GdVO_4$ (6 cm^{-1} for π and σ polarizations, respectively) [7] and the widely used 1.0 at.% Nd^{3+}:YAG (8 cm^{-1}) [13] crystal at 808 nm. The gain medium with large absorption coefficient at the pump wavelength can absorb the pumping light from LD effectively in a small thickness, and then the laser threshold can be reduced. Therefore, the Tm^{3+}:BGM cleavage plate is a promising gain medium for LD pumping around 808 nm.

Excited by a Ti:sapphire laser at 798 nm (Model 3900s, Spectra-Physics), the room-temperature polarized fluorescence spectra of the $^3F_4 \rightarrow {}^3H_6$ transition of Tm^{3+} ions in the BGM cleavage plate were recorded using a monochromator (Triax550, Jobin-Yvon) with a thermoelectrically cooled PbS detector (DSS-PS020T, Jobin-Yvon). Broad emission bands up to 2050 nm with full widths at half the maximum of about 170 nm were observed for both polarizations. Figure 2 shows the normalized polarized fluorescence spectra in a range of 1600–2100 nm.

3 Laser experiment

The schematic diagrams of experimental setups are depicted in Fig. 3. The laser experiment was carried out in end-pumped linear resonators. A home-made single-stripe AlGaAs LD, in which diode module was manufactured by the Premier Opto-electronics Technology Co., Ltd., was used as the pump source. By adjusting the operating temperature of the diode module, the emitting wavelength of the LD was

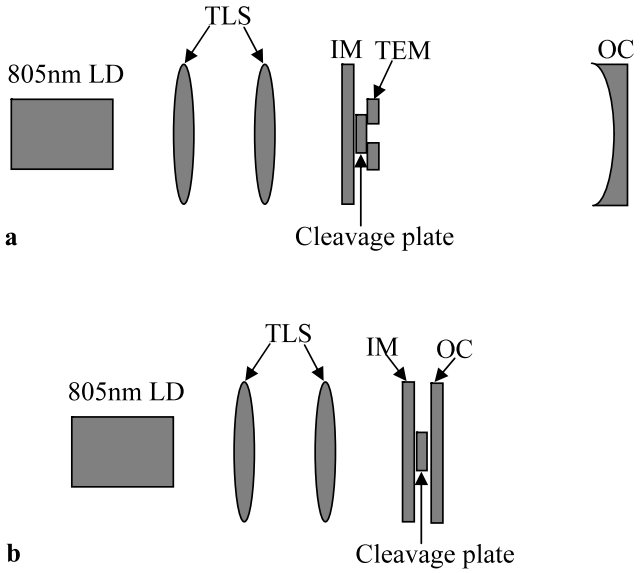

Fig. 3 Schematic diagrams of experimental setups: (**a**) hemispherical cavity. The distance between IM and OC is about 50 mm; (**b**) plano–plano cavity. The distance between IM and OC is about 4 mm

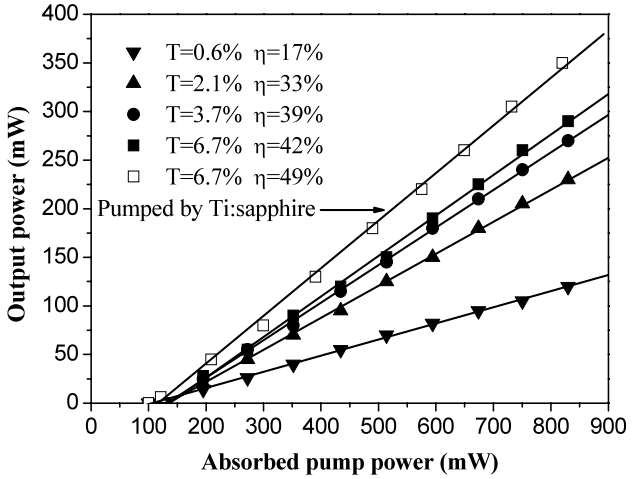

Fig. 4 CW 2-μm output power of the Tm^{3+}:BGM laser pumped by diode laser at 805 nm versus absorbed pump power for different transmissions T of output couplers in a hemispherical cavity. CW output power of the Tm^{3+}:BGM laser pumped by Ti:sapphire laser at 805 nm for the output coupler with transmission of 6.7% is also shown (*open square*)

tuned to 805 nm. After passing a simple telescopic lens system (TLS), the pump beam was focused to be a rectangle-shape with size of 30 × 110 μm^2 in the Tm^{3+}:BGM cleavage plate. The polarization of the pump light was parallel to the Z axis of the plate. The plate was not antireflection coated and attached to an aluminum slab with a heat-conducting adhesive. The temperature of the aluminum slab was controlled by an air-cooled Peltier thermoelectric module (TEM) and kept at about 15°C during laser operation. In the center of the slab and TEM, there is a hole for the passing of the pump beam and fundamental laser. The input mirror (IM) had 90% transmission at 805 nm and 99.8% reflectivity in a range of 1900−2000 nm. For the hemispherical cavity, four output couplers (OCs) with a fixed 50-mm radius of curvature (RoC) and different transmissions (0.6%, 2.1%, 3.7%, and 6.7%) in the range of 1900−2000 nm were used. In order to reduce the cavity loss, the length of the hemispherical cavity was set near to the RoC of the output couplers. For the plano–plano cavity, three flat OCs with different transmissions (1.1%, 2.1%, and 3.8%) in the range of 1900–2000 nm were used. The cavity length was kept at about 4 mm. The TEM was not used in the plano–plano cavity because it lengthens the cavity and then suppresses the laser oscillation. The reflectivities of all the output couplers at 805 nm were higher than 99%. From the thickness of 1.6 mm and the absorption coefficient of about 6.0 cm^{-1} at 805 nm, about 60% of the incident pump power was absorbed by the cleavage plate under no lasing condition.

4 Results and discussion

Figure 4 shows the dependence of the measured 2-μm CW output power of the diode-pumped Tm^{3+}:BGM laser on the absorbed pump power at 805 nm for different OCs in the hemispherical cavity. Due to the low threshold of the Tm^{3+}:BGM laser and the low pump power used in this work, only a small part of Tm^{3+} ions was excited into the upper laser level. Therefore, the absorption efficiency (about 60%) of the cleavage plate obtained under no lasing condition was adopted approximately for that under lasing condition. Then, by measuring the pump laser power after IM, the absorbed pump power can be estimated when the reflectivity (about 10% calculated from the refractive index of about 2 for the BGM crystal [14]) of the crystal surface and the absorption efficiency of the cleavage plate were taken into account. For the OC with transmission of 0.6%, the absorbed pump threshold was 100 mW, and the maximum output power of 120 mW with slope efficiency of 17% was obtained when the absorbed pump power was 830 mW. For the OC with transmission of 6.7%, the absorbed pump threshold, the maximum output power, and the slope efficiency increased to 130 mW, 290 mW, and 42%, respectively. The amplitude instability of the output power was measured to be less than ±2.0% in a 10-min period. The highest slope efficiency of 42% obtained in the Tm^{3+}:BGM cleavage plate is among those of Tm^{3+}:$GdVO_4$ (28%) [7], Yb^{3+}:Tm^{3+}:$KY(WO_4)_2$ (52%) [3], and Tm^{3+}:$KY(WO_4)_2$ (53%) [15] crystals pumped by LD around 805 nm. The obtained slope efficiency is very close to its Stokes limit (about 40%), which shows that the cross-relaxation process also exists in the 7.2 at.% Tm^{3+}:BGM crystal. Furthermore, it can

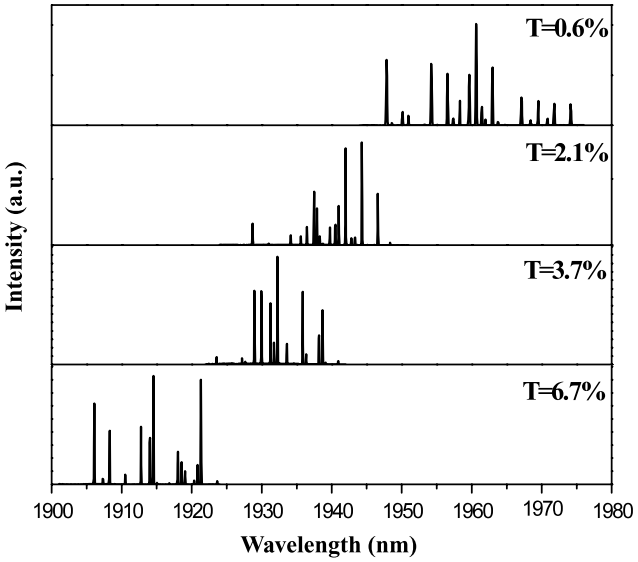

Fig. 5 Spectra of the Tm^{3+}:BGM laser when absorbed pump power is 830 mW for different output coupler transmissions T in a hemispherical cavity

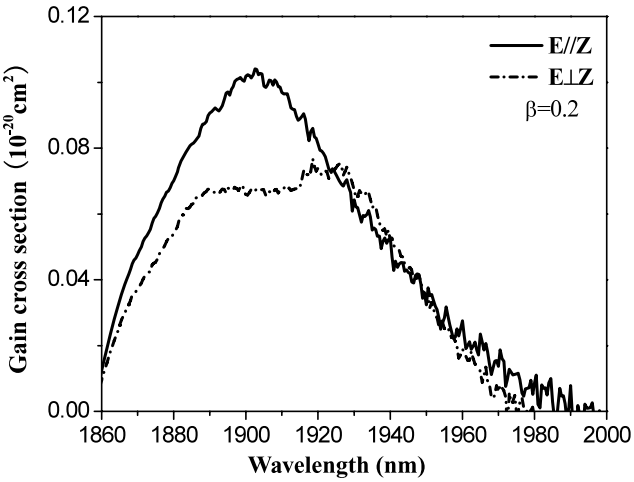

Fig. 6 Room-temperature polarized gain cross-section spectra for the $^3F_4 \rightarrow {}^3H_6$ transition of the Tm^{3+}:BGM cleavage plate when the population inversion ratio is 0.2

be seen from the figure that the output power is not saturated at the maximum absorbed pump power for all the OCs, which indicates that the cleavage plate can be effectively cooled and higher output power can be achieved when the pump power is increased. Moreover, the laser performance of the Tm^{3+}:BGM plate may be also further improved by optimizing the OC transmission.

The laser performance of the Tm^{3+}:BGM cleavage plate pumped by a CW Ti:sapphire tunable laser (Model 3900s, Spectra-Physics) at 805 nm was also investigated in the similar experimental scheme. The beam radius of the Ti:sapphire laser with TEM_{00} mode, which has better beam quality than that of the home-made single-stripe LD used above, was focused to be about 20 μm in the plate. The experimental result for the OC with transmission of 6.7% is also shown in Fig. 4. When the absorbed pump power was 820 mW, the achieved maximum output power, absorbed pump threshold, and slope efficiency were 350 mW, 100 mW, and 49%, respectively. The slope efficiency is close to that obtained previously in a 1.1-mm-thick Tm^{3+}:BGM cleavage plate pumped at 798 nm (51%) [11]. Comparing the experimental results obtained in the case of LD and Ti:sapphire laser pumping, it can be seen that the laser performance of the diode-pumped Tm^{3+}:BGM cleavage plate can be improved when the output beam quality of LD is optimized.

When the absorbed pump power was 830 mW, the spectra of the diode-pumped Tm^{3+}:BGM laser for different OC transmissions in the hemispherical cavity were recorded with a monochromator (Triax550, Jobin-Yvon) and are shown in Fig. 5. Similar to the results obtained in the 1.1-mm-thick Tm^{3+}:BGM cleavage plate pumped by Ti:sapphire laser at 798 nm [11], the central wavelength of laser oscillation blue-shifted from 1960 to 1915 nm when the OC transmission increased from 0.6% to 6.7%. The polarization of output beam was also measured at all absorbed pump power for different OC transmissions. For the OCs with transmissions of 0.6% and 6.7%, the polarization of output laser of the Tm^{3+}:BGM plate was totally linear and parallel to the Z axis of the plate. However, for the OCs with medium transmissions of 2.1% and 3.7%, the polarization of output laser was not totally linear, and the ratio of the output power of fundamental laser between $E \perp Z$ and $E \parallel Z$ was larger than 10.

The above phenomenon may be caused by the difference of the polarized gain cross-section at oscillating wavelength for different OC transmissions. As an example, the room-temperature polarized gain cross-section spectra for the $^3F_4 \rightarrow {}^3H_6$ transition of Tm^{3+} ions in the BGM cleavage plate are shown in Fig. 6 when the population inversion ratio β is 0.2. The gain cross-sections were obtained from the measured absorption spectra of the $^3H_6 \rightarrow {}^3F_4$ transition and emission cross-sections calculated by the reciprocity method [16]. The calculating process is similar to that reported in Ref. [11]. Although the signal-to-noise ratio of the gain cross-section spectra at wavelength longer than 1900 nm is low, which are originated from the weak absorption of the plate in this region and then exponentially expanded in the calculation of the emission cross-sections [17], the change trend of the polarized gain cross-section with wavelength is obvious. At wavelengths shorter than 1920 nm and longer than 1950 nm, which are the oscillating wavelengths for the OCs with transmissions of 6.7% and 0.6%, respectively, the gain cross-sections for $E \parallel Z$ are larger than those for $E \perp Z$, which is in favor of the generation of the linearly polarized laser for $E \parallel Z$. The linearly po-

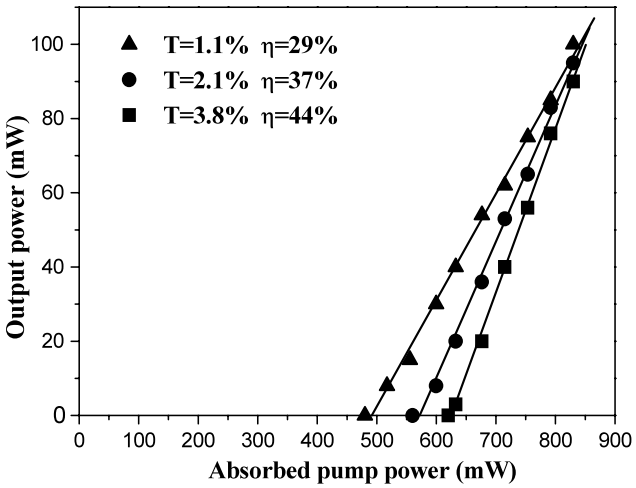

Fig. 7 CW 2-μm output power of the Tm^{3+}:BGM laser pumped by diode laser at 805 nm versus absorbed pump power for different transmissions T of output couplers in a plano–plano cavity

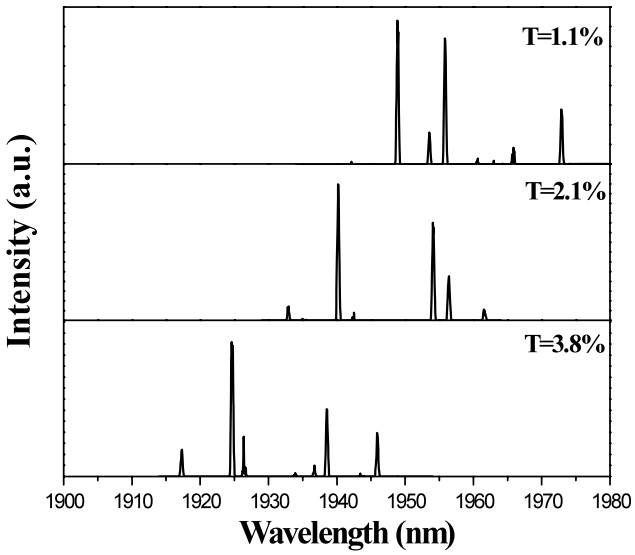

Fig. 8 Spectra of the Tm^{3+}:BGM laser when absorbed pump power is 830 mW for different output coupler transmissions T in a plano–plano cavity

larized laser is useful for some applications, such as stimulated Raman shift [18] and optical parametric oscillator [19] for obtaining valuable laser at other wavelength. However, at wavelengths between 1920 and 1950 nm, which are the oscillating wavelengths for the OCs with transmissions of 2.1% and 3.7%, the case is reversal. The slightly larger gain cross-section for $E \perp Z$ causes the generation of the polarized laser with not totally linear nature.

Figure 7 shows the measured laser output power of diode-pumped Tm^{3+}:BGM cleavage plate as a function of the absorbed pump power in the plano–plano cavity. For the OC with transmission of 1.1%, the achieved maximum output power was 100 mW when the absorbed pump power was 830 mW. The absorbed pump threshold was 480 mW, and slope efficiency was 29%. When the OC transmission increased to 3.8%, the absorbed pump threshold, the maximum output power, and the slope efficiency were 620 mW, 90 mW, and 44%, respectively. The amplitude instability of the output power was measured to be about ±5.0% in a 10-min period, which is higher than that recorded in the hemispherical cavity because the temperature of the plate cannot be controlled by the TEM in this case. For the similar OC transmission, the higher threshold and slope efficiency obtained in the plano–plano cavity than those in the hemispherical one may be caused by the larger cavity loss and the better matching between pump and laser modes, respectively. Consequently, it can be expected that when the cavity mirrors are directly deposited onto the surfaces of cleavage plate, an efficient diode-pumped monolithic 2-μm laser can be realized [20].

The laser spectra at the absorbed pump power of 830 mW in the plano–plano cavity are shown in Fig. 8. The variation trend of the spectra with the OC transmission is similar to that in the hemispherical cavity. However, for the similar OC transmission, the reduced number of the longitudinal modes in the plano–plano cavity is caused by the larger cavity loss, lower output power, and shorter resonator length. The polarization of the output laser beam for all the OCs was measured to be totally linear and parallel to the Z axis of the plate in the plano–plano cavity. The variation of beam polarization for different OCs recorded in the hemispherical cavity was not observed, and it may be caused by the strong thermal effect of the uncooled plate.

Obvious upconversion visible fluorescence of the Tm^{3+}:BGM plate was observed by naked eyes during the laser operation and the unpolarized spectrum excited at 805 nm is shown in Fig. 9. There are five fluorescence bands located around 480, 530, 550, 660, and 690 nm in the spectrum. By a two-photon absorption process, the ground state Tm^{3+} ions can be excited into the $^1G_4$ multiplet and then partly populated in the $^3F_2$ and $^3F_3(^3F_{2,3})$ multiplets via nonradiative relaxation. Then, the transitions of $^1G_4 \rightarrow {}^3H_6$, $^1G_4 \rightarrow {}^3F_4$, and $^3F_{2,3} \rightarrow {}^3H_6$ are responsible for the blue and red upconversion fluorescence around 480, 660, and 690 nm, respectively [21]. Furthermore, by comparing the spectra recorded in the cleavage plate and in some Er^{3+}-doped crystals [22, 23], it can be deduced that the green upconversion fluorescence around 530 and 550 nm are corresponding to the $^2H_{11/2} \rightarrow {}^4I_{15/2}$ and $^4S_{3/2} \rightarrow {}^4I_{15/2}$ transitions of Er^{3+} ions, respectively, which are impurities in the Tm_2O_3 raw material. Many investigations have shown that the upconversion will reduce the population at the upper laser level and increase the thermal load in the gain medium [24, 25], and then decrease the fundamental laser performance. Therefore, by optimizing the Tm^{3+} concentration in the BGM crystal to weaken the upconversion and using a Tm_2O_3 raw

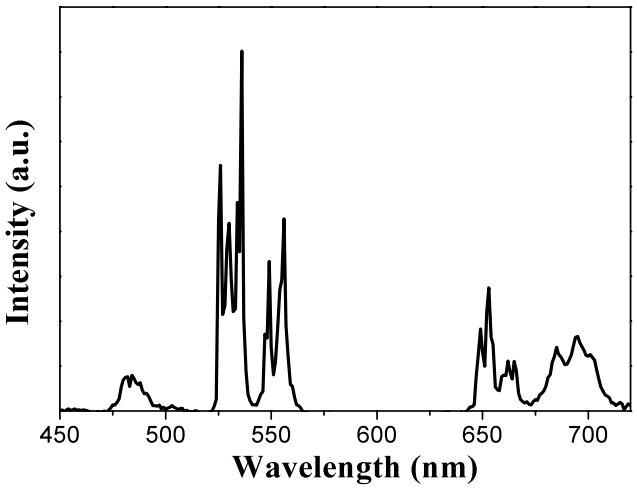

Fig. 9 Unpolarized upconversion fluorescence spectrum of the 7.2 at.% Tm^{3+}:BGM cleavage plate in a range of 450–720 nm. The exciting wavelength is 805 nm

material with higher purity for growing the crystal, the laser performance of the Tm^{3+}:BGM plate could be further improved.

5 Conclusions

Using an unprocessed 1.6-mm-thick, 7.2 at.% Tm^{3+}:BGM cleavage plate as gain medium, efficient CW 2-μm laser operation was demonstrated when it was end-pumped by an 805-nm single-stripe LD. At the absorbed pump power of 830 mW, a maximum output power of 290 mW with slope efficiency of 42% and 90 mW with slope efficiency of 44% were realized in the hemispherical and plano-plano cavities, respectively. The polarization of output laser for different OC transmissions was also analyzed in detail. The investigations show that optimizing the beam quality of pump source and the Tm^{3+} concentration and eliminating the Er^{3+} impurity in the crystal are the important ways to improve the laser performance of the Tm^{3+}:BGM cleavage plate. Since the absorption coefficient at 808 nm is close to that at 805 nm for $E \parallel Z$, the experimental results of this work reveal that the Tm^{3+}:BGM cleavage plate is a promising 2-μm laser gain medium pumped by the widely used LD around 808 nm.

Acknowledgements This work has been supported by the National Natural Science Foundation of China (grants 50590405 and 50802094), the Major Programs of the Chinese Academy of Sciences (grant SZD08001-1), the Knowledge Innovation Program of the Chinese Academy of Sciences, and the Fund of National Engineering Research Center for Optoelectronic Crystalline Materials (grant 2005DC105003).

References

1. M. Eichhorn, Appl. Phys. B **93**, 269 (2008)
2. X. Mateos, V. Petrov, J. Liu, M. Pujol, U. Griebner, M. Aguilo, F. Diaz, M. Galan, G. Viera, IEEE J. Quantum Electron. **42**, 1008 (2006)
3. L.E. Batay, A.A. Demidovich, A.N. Kuzmin, A.N. Titov, M. Mond, S. Kuck, Appl. Phys. B **75**, 457 (2002)
4. F. Cornacchia, D. Parisi, C. Bernardini, A. Toncelli, M. Tonelli, Opt. Express **12**, 1982 (2004)
5. N. Coluccelli, G. Galzerano, P. Laporta, F. Cornacchia, D. Parisi, M. Tonelli, Opt. Lett. **32**, 2040 (2007)
6. C. Li, J. Song, D. Shen, N.S. Kim, K. Ueda, Y. Huo, S. He, Y. Cao, Opt. Express **4**, 12 (1999)
7. Y. Urata, S. Wada, Appl. Opt. **44**, 3087 (2005)
8. E.C. Honea, R.J. Beach, S.B. Sutton, J.A. Speth, S.C. Mitchell, J.A. Skidmore, M.A. Emanuel, S.A. Payne, IEEE J. Quantum Electron. **33**, 1592 (1997)
9. V.V. Vakulyuk, A.A. Evdokimov, G.P. Khomchenko, Russ. J. Inorg. Chem. **27**, 1016 (1982)
10. D. Zhao, Z. Lin, L. Zhang, G. Wang, J. Phys. D: Appl. Phys. **40**, 1018 (2007)
11. H. Zhu, Y. Chen, Y. Lin, X. Gong, Z. Luo, Y. Huang, J. Opt. Soc. Am. B **25**, 801 (2008)
12. N.I. Borodin, P.V. Kryukov, A.V. Popov, S.N. Ushakov, A.V. Shestakov, Quantum Electron. **35**, 511 (2005)
13. L. DeShazer, Laser Focus World **30**, 88 (1994)
14. N.F. Fedorov, V.V. Ipatov, G.I. Rozhnovskaya, Russ. J. Inorg. Chem. **27**, 1019 (1982)
15. A.E. Troshin, V.E. Kisel, A.S. Yasukevich, N.V. Kuleshov, A.A. Pavlyuk, E.B. Dunina, A.A. Kornienko, Appl. Phys. B **86**, 287 (2007)
16. D.E. McCumber, Phys. Rev. **136**, A954 (1964)
17. R.M. Martin, R.S. Quimby, J. Opt. Soc. Am. B **23**, 1770 (2006)
18. L.E. Batay, A.N. Kuzmin, A.S. Grabtchikov, V.A. Lisinetskii, V.A. Orlovich, A.A. Demidovich, A.N. Titov, V.V. Badikov, S.G. Sheina, V.L. Panyutin, M. Mond, S. Kuck, Appl. Phys. Lett. **81**, 2926 (2002)
19. D. Creeden, P.A. Ketteridge, P.A. Budni, S.D. Setzler, Y.E. Young, J.C. McCarthy, K. Zawilski, P.G. Schunemann, T.M. Pollak, E.P. Chicklis, M. Jiang, Opt. Lett. **33**, 315 (2008)
20. G.J. Koch, J.P. Deyst, M.E. Storm, Opt. Lett. **18**, 1235 (1993)
21. O. Silvestre, M.C. Pujol, M. Rico, F. Guell, M. Aguilo, F. Diaz, Appl. Phys. B **87**, 707 (2007)
22. X. Gong, Y. Lin, Y. Chen, J. Liao, X. Chen, Z. Luo, Y. Huang, Appl. Phys. B **91**, 499 (2008)
23. D. Wang, M. Yin, S. Xia, V.N. Makhov, N.M. Khaidukov, J.C. Krupa, J. Alloys Compd. **368**, 337 (2004)
24. X. Zhang, Y. Wang, L. Li, Y. Ju, J. Phys. D: Appl. Phys. **40**, 6930 (2007)
25. S. Bjurshagen, R. Koch, Appl. Opt. **43**, 4753 (2004)